Response to reviewer 1

Reviewer's comments are in blue, our responses are in black

The authors reported on the measurement results of natural and artificial ice layer densities in the snowpack using a new field measurement technique. They also discussed the errors resulting from their technique in detail. Thus, their results should be more certain than the previous studies. Because the number of observations is too small, the work does not present completely innovative results, but rather presents an incremental advance in a technique to measure accurate density of ice layer in the snowpack. From this viewpoint, this paper is worth publishing in TC. However, I think there are several points to clear before publication. Below I give suggestions on improvements for better understanding the arguments in the manuscript.

We are glad that the reviewer recognises the importance of improvements in this area. In the discussion we refer to future work to further increase the number of measurements of ice layer density and hope that this publication will encourage others to apply this method too.

L94-96: How was the mean squared error in the measurement of the ice sample volume calculated? Please add more detail explanation.

Added ($error = \sqrt{0.125^2 + 0.125^2}$) so the sentence now reads:

"Based on carrying out 10 repeat measurements on 10 centrifuge tube photos the (mean) error was found to be ± 0.125 cm^3 in each photo of the ice sample volume equating to a root mean squared error in the measuremnet of the ice sample volume of ± 0.18cm^3 ($error = \sqrt{0.125^2 + 0.125^2}$), as each volume measurement involves reading the volume from two photos."""

L147: How was the random error in the density measurements calculated? Please add more detail explanation.

The random error in density was calculated by applying the random error in the volume measurements (0.18 cm^3) to the bias corrected volume of the sample and calculating the minimum and maximum mean density. When looking at the field measurements in order to clarify this point I noticed that while the mean density had been correctly calculated using the bias corrected values the random error in density had not been calculated using the bias corrected values. As a result overall uncertainty in the density measurements is ± 28 kg m^{-3} rather than ± 18 kg m^{-3}. This makes no difference to the conclusions or outcomes of this paper and has been changed throughout the manuscript.

In response to the reviewer's comment this section has been updated to read:

"After measurements were corrected for bias the mean sample volume was 6.4 cm^3, when the random error of ± 0.18 cm^3 was applied to the volume measurements an uncertainty of ± 28 kg m^{-3} was calculated"

L157 & Table 3: The explanation of Table 3 is insufficient. What is n in the Table 3? If n indicates the measurement number, what does n¡0. 1 mean? Please add more detail explanation.

Updated caption to:

"Measurements of ice layer bubble size and ice layer thickness (all sizes in mm). n is number of samples, $n < 0.1$ is the number of bubbles with diameter of less than 0.1 mm."

L181 & Fig. 4: Is the simulation results of 800 kg m-3 in Fig. 4 true? The areas replaced by bubbles in the figure seem to be much larger than those supposed from its density. The simulation results should depend on the initial pure ice density, which does not have any bubbles. Thus, please add the explanation of the initial pure ice density in the simulation.

The appearance of having too many bubbles is a function of the viewing angle of the cube - i.e. bubbles in the foreground will shadow ice behind it hence giving the impression there are too many bubbles, despite the fact it's correct. To clarify the issue of the initial pure ice density line 181 was updated to:

"After each sphere was placed, the total volume of all the spheres and the density of the ice sample was calculated. Spheres were added to the sample until the desired density was reached starting from an initial pure ice density of 916 kg m^{-3}."

L202: Do you think the dependence of pure ice density on temperature is enough strong to affect the density difference between artificial and natural ice layer? As shown in Table1, the density difference between the 0°C and -40° C is less than 7 kg m^{-3}. Please add the detail explanation if you have any idea to support your hypothesis.

We estimate the maximum possible variation in ice layer temperature for our data to be less than 20°C, which represents a density variation of less than 2 kg m^{-3}. While there is potential for this to have a small impact we do not have field data of ice layer temperatures and are therefore unable to constrain the error. We recognise that there is potential that this could have an impact on measurement accuracy and as a result this is mentioned in the discussion.

Response to Reviewer 2

Reviewers comments are in blue, our responses are in black

The need to account accurately for the density of ice layers is evident from the introductory review of this paper. As no reliable method is available at present, the authors present a novel, simple, and promising method to measure the density of thin ice layers. They also took care to present a thorough error analysis, which is an asset. In addition, the paper reads nicely except for the section on effective porosity that would benefit from some re-visiting by the authors. However, the method was so far applied to 4 ice layers only, two of which were artificial. It is thus questionable whether it can already be seen as a standard and can be part of the special issue Intercomparison of methods to characterise snow microstructure without prior proper comparison with another method, as proposed by the authors themselves. I recommend accepting the paper after the authors addressed the porosity issue and do some minor revisions as suggested below. Whether it is included in the special issue is left to the appreciation of the editor

Thank you for your comments.

p. 5983, line 12: why volume range?

We agree with the reviewer that it not a range, it is a single value with uncertainty. The term "range" has been deleted.

p. 5984, line 16: Consequently . . . Im not sure this is the correct statement. You found your method to be accurate to 4 %. Whether this is low enough will depend on the application.

We agree. This statement has been removed.

p. 5984, line 18: Field measurements: how were the samples taken and cleared from surrounding snow?

I have added the sentence:

"Ice layers were removed from the surrounding snow and broken to size using a scraper."

p. 5984, line 28: To create the . . . unclear! Was the melt-freeze crust in the end part of the ice layer?

The following was added to the paragraph:

"After the removal of recent snow, water was sprayed onto the snowpack to create a surface ice layer. The ice layer was distinct to the melt-freeze crust and was removed when the layer was extracted."

p. 5985, line 21: thickness gradient Could you indicate the range in numbers?

Changed to:

"Water was sprayed over an area of 1 m^2, concentrating the spraying towards one edge, creating ice thicknesses between 1 and 6 mm which allowed 28 measurements of ice layer density across a range of ice layer thicknesses."

Natural ice layers . . . Are the two distributions not significantly different? Of course, the statement would still rely on 2 ice layers each!

Added:

"analysis using the Kolmogorov-Smirnov test showed all ice layers to be significantly different."

physically reasonable From Table 2, the mean of 915 kg m^{-3} does not seem less reasonable than from the artificial layer at North Bay!

Changed to:

"The measurements in Inuvik were made outside, and whilst care was taken to ensure the balance was level and condensation was cleaned from the balance as it formed, these cannot be ruled out as sources of error and could be a reason why some of the high outlying measured densities (Figure 3) are physically unreasonable at the Inuvik site."

effective porosity Is this the proper term?

In this section both effective porosity and volume error from porosity have been used interchangeably. We have corrected this by adding:

(p5988 l9) "As the density of the sample decreased volume error from porosity in the sample ranged from 6.5×10^{-5} to 1×10^{-3} cm^3."

Why in cm^3 (porosity has no dimension).

When effectivity porosity is being referred to the units have been removed, the following changes have also been made:

1. (p5987 l6) "However, due to the presence of bubbles in the ice layers some increase in porosity would occur as more bubbles are exposed when the ice layer was broken and placed in the centrifuge tube. The exposure of the bubbles causes effective porosity and is represented by a dimensionless decimal fraction which represents the proportion of a volume which is available for liquid to flow through."

2. Figure 6 axis updated

Are you not rather decreasing the porosity by breaking the sample in pieces?

Breaking the ice layer will expose more bubbles at the edge of the sample, the following sentence has been updated:

(p5987 l6) "However, due to the presence of bubbles in the ice layers some increase in porosity would occur as more bubbles are exposed when the ice layer was broken and placed in the centrifuge tube. The exposure of the bubbles causes effective porosity and is represented by a dimensionless decimal fraction which represents the proportion of a volume which is available for liquid to flow through."

This has been updated to:

"Air bubbles within the ice layer were represented using spheres, scattered randomly without any overlap, within an ice sample of size x, y, z and density d. The sizes of the spheres were determined by taking a random sample from a normal distribution of bubble sizes based on the mean and standard deviation of bubble diameter measurements. A sphere size was chosen randomly from the distribution and located randomly within the x, y, z axes. If the sphere overlapped another sphere then the location was changed until no overlap occurred."

Figure 6: effect Can we really speak of an effect here?

Changed to: Sample density vs mean simulated sample porosity (Blue line).

Improved measurement of ice layer density in seasonal snowpacks

T. Watts[1], N. Rutter[1], P. Toose[2], C. Derksen[2], M. Sandells[3,a], and J. Woodward[1]

[1]Department of Geography, Northumbria University, Newcastle upon Tyne, NE1 8ST, UK
[2]Climate Research Division, Environment Canada, Toronto, Canada
[3]National Centre for Earth Observation, University of Reading, Reading, RG6 6AL, UK
[a]now at: CORES Science and Engineering Limited, Victoria Garesfield, UK

Correspondence to: N. Rutter (nick.rutter@northumbria.ac.uk)

Abstract. Ice layers in snowpacks introduce uncertainty in satellite derived estimates of snow water equivalent, have ecological impacts on plants and animals, and change the thermal and vapour transport properties of the snowpack. The microstructure and specifically the density of ice layers is poorly quantified. Here we present a new field method, for measuring the density of ice layers caused by melt or rain-on-snow events. The method was used on 87 ice layer samples in the Canadian Arctic and mid-latitudes; the mean measured ice layer density was $909 \pm \text{18}28 \, \mathrm{kg \, m^{-3}}$ with a standard deviation of $23 \, \mathrm{kg \, m^{-3}}$, significantly higher than values typically used in the literature.

1 Introduction

Ice structures form in snowpacks during melt or rain-on-snow events (Colbeck, 1991). Rain either freezes on contact with the surface of the snowpack, or water refreezes within the snowpack to form ice layers, lenses, crusts, columns, or basal ice layers (Gray and Male, 1981). Strong intercrystalline bonds created from refreezing of liquid water, lead to the formation of cohesive ice structures (Fierz et al., 2009). The presence of ice layers changes the thermal and vapour transport properties of the snowpack, which increases soil temperature (Putkonen and Roe, 2003), and encourages the growth of fungus and molds that lead ungulate deaths (Kumpula et al., 2000). Additionally the physical barrier to subnivean vegetation presented by ice layers in the snowpack is linked with a large reduction in ungulate survival via starvation and reduced calf production rate (Grenfell and Putkonen, 2008). Permeability of ice layers to liquid water and gas is vastly reduced compared to snow (Albert and Perron Jr., 2000; Colbeck and Anderson, 1982; Keegan et al., 2014). Impermeable layers are identifiable because pores do not connect within the ice formation, and the granular snowpack structure is missing (Fierz et al., 2009). Ice layers differ from ice crusts and ice lenses; ice crusts are always permeable and have a coarse grained granular snow-like structure (Colbeck and Anderson, 1982). Ice lenses can be impermeable, do not have a granular structure and are spatially discontinuous. Sim-

ilarly to ice lenses, ice layers can be impermeable, and do not have a granular structure, however, ice layers are continuous (Fierz et al., 2009).

Ice layers introduce uncertainty into the performance of snow microwave emission models (Rees et al., 2010), which are an important component of satellite derived snow water equivalent (SWE) retrieval algorithms (Takala et al., 2011). The radiometric influence of thin ice layers poses a significant challenge for physical and semi-empirical emission models, which can either treat ice layers as coarse grained snow (Mätzler and Wiesmann, 1999) or as planar (flat and smooth) ice layers (Lemmetyinen et al., 2010).

As the climate warms, an increase in the number of mid-season melt and rain-on-snow events is predicted (Putkonen and Roe, 2003), which will likely increase the occurrence of ice layers in the Arctic (Ye et al., 2008) and mid-latitudes (Freudiger et al., 2014). The microstructure and properties of ice layers remain poorly quantified with field observations, which hinders snow emission model development and evaluation (Montpetit et al., 2012). Durand et al. (2008) carried out sensitivity studies and simulations of mountain snowpack brightness temperature with the Microwave Emission Model of Layered Snowpacks (MEMLS) (Wiesmann and Mätzler, 1999). The lack of an accurate ice layer density measurement technique, meant that the uncertainties attributed to not knowing the density of ice layers were 32.2 and 15.3 K for horizontally polarised (H-pol) 18.7 and 36.5 GHz frequencies respectively, a greater uncertainty than any other parameter investigated (Durand et al., 2008).

Pure ice density ranges from $916 \, \mathrm{kg \, m^{-3}}$ at $0 \, °C$ to $922 \, \mathrm{kg \, m^{-3}}$ at $-40 \, °C$ (Table 1). Only limited field measurements of ice layer densities have previously been attempted. Ice layer density measurements taken in the Canadian Arctic by submerging pieces of ice crust into oil resulted in a range of densities from 630 to $950 \, \mathrm{kg \, m^{-3}}$ (Marsh, 1984). Ice layer densities of 400 to $800 \, \mathrm{kg \, m^{-3}}$ were measured using a snow fork (which measures the dielectric properties of snow around 1 GHz (Sihvola and Tiuri, 1986)) in seasonal snow on the Greenland ice sheet (Pfeffer and Humphrey, 1996). The results from these studies vary drastically and a quantitative assessment of the error in measurement techniques is absent. Consequently, the aim of this paper is to describe a newly developed field measurement technique for measuring ice layer density, and present density measurements made in Arctic and mid-latitude snowpacks.

2 Method

2.1 Development of ice density measurement method

A new laboratory and field-based method was developed to measure the density of ice layers found in seasonal snow, based on volumetric displacement. The basic principle is that when an ice layer sample is submerged in a vessel of liquid, calculating the volume displacement and sample mass will yield an estimate of density. The laboratory and field protocols for measuring the density of ice

2

layers with this method is outlined in Fig. 1. The mass of a sealed $50\,\text{mL}$ centrifuge tube with $2.5\,\text{mL}$
graduations containing white spirit (sometimes termed "mineral spirits"), was measured with a precision of $\pm0.001\,\text{g}$ under laboratory conditions before entering the field. White spirit is immiscible with water and has a low freezing point ($-70\,°\text{C}$), eliminating potential sample melt. White spirit also has a low density ($650\,\text{kg}\,\text{m}^{-3}$), making it likely that the ice sample would sink and be completely submerged. In the field the centrifuge tube was held by a fixed, levelled, mounting system within the macro setting range of a compact camera. Each camera image was centred on a visible datum on the mounting system to ensure the camera was correctly focused, and that repeat images were consistently made from the same horizontal position. Images were taken before and after each ice sample was submerged as shown in Fig. 2.

In each image three positions were identified during post processing: the liquid level, the graduation above the liquid level and the graduation below the liquid level. Pixel co-ordinates of these positions were recorded and the proportional height of the liquid level between the upper and lower graduation was translated to a volume at a higher resolution than the centrifuge tube graduations alone would allow. The top of the liquid level was located rather than the meniscus for ease of identification; as relative volume change was used no error was introduced. After images were taken, the centrifuge tube containing the sample was sealed and the change in mass was measured on return to the laboratory. Only samples where the liquid in the tube was level in both images were considered.

2.2 Methodological error

Ice layers found in snowpacks are very difficult to accurately and consistently re-create under laboratory conditions. Therefore to assess the accuracy of the ice density measurement technique, ball bearings of known volume were measured. Stainless steel ball bearings were used (manufactured to a diameter of $1\pm2.5\times10^{-5}\,\text{cm}$), resulting in a volume ~~range~~ of $0.5236\pm0.0004\,\text{cm}^3$. The volume of the ball bearings was calculated from before and after images of 10 ball bearings submerged in the centrifuge tube. The expected total volume of all ball bearings of approximately $5.236\,\text{cm}^3$ is comparable to the mean volume of ice samples ~~collected~~collected. Of 134 samples, each consisting of 10 ball bearings, the mean volume was $5.045\,\text{cm}^3$. The volume measurements were normally distributed and an error value based on ±1 standard deviations was calculated, resulting in a systematic volume measurement error or bias of $-0.19\,\text{cm}^3$.

The largest source of error is in reading the height of the liquid in the centrifuge tube from the camera photos. Identifying the precise height of the surface of the liquid between the graduation markings on the cylinder is limited by the quality of the camera focus and resolution of the camera. If the camera focus is not perfect it is difficult to locate the height of the liquid, which result in error and uncertainty. Based on carrying out 10 repeat measurements on 10 centrifuge tube photos the (mean) error was found to be $\pm0.125\,\text{cm}^3$ in each volume measurement photo, equating to a ~~~~random root mean squared error in the measurement of the ice sample volume of $\pm0.18\,\text{cm}^3$

3

95    $(error = \sqrt{0.125^2 + 0.125^2})$, as each volume measurement involves reading the volume from two photos.

     To calculate the optimum sample volume the number of ball bearings used in each volume measurement was increased from 1 to 24, a volume range of 0.52 to $12.57\,\mathrm{cm}^3$. Correlation between standard deviation and sample volume was not statistically significant (confidence $> 99\%$), demon-

100   strating that the error in volume measurement was independent of sample volume. Field trials suggested that $10\,\mathrm{cm}^3$ was the maximum sample volume routinely possible to use due to the diameter of the centrifuge tube. Although no minimum sample volume was set, the largest possible sample was obtained.

     To estimate the potential impact of the uncertainty in volume measurement on samples taken

105   in the field, the random ($\pm 0.18\,\mathrm{cm}^3$) volume measurement error from the ball bearing experiment was applied to a theoretical ice sample of volume $4.89\,\mathrm{cm}^3$ and mass $4.53\,\mathrm{g}$ (equating to a density of $916\,\mathrm{kg\,m}^{-3}$). This volume error from the ball bearing experiment translated into an observed volume ~~range~~ of 4.53–$4.89\,\mathrm{cm}^3$ (i.e. $4.71 \pm 0.18\,\mathrm{cm}^3$). Assuming no error in the mass balance (precision of $\pm 0.001\,\mathrm{g}$), the upper density value (minimum volume) was $951\,\mathrm{kg\,m}^{-3}$ and the lower density

110   value (maximum volume) was $881\,\mathrm{kg\,m}^{-3}$, representing an uncertainty in density of $\pm 35\,\mathrm{kg\,m}^{-3}$ or 4%. ~~Consequently, the impact of the error was estimated to be low enough to justify the practical application of this technique.~~

2.3   Field measurements

During the winter of 2013, ice layer density measurements were collected at three sites in Canada:

115   North Bay, Ontario ($46.33°\,\mathrm{N}$, $79.31°\,\mathrm{W}$) between 8–9 February, Canadian Centre for Atmospheric Research (CARE), Egbert, Ontario ($44.23°\,\mathrm{N}$, $79.78°\,\mathrm{W}$) on 25 February, and Trail Valley Creek, Inuvik, North West Territories ($68.72°\,\mathrm{N}$, $133.16°\,\mathrm{W}$) on 9 April. Ice layers were removed from the surrounding snow and broken to size using a scraper.

     In North Bay, snow stratigraphy, density and the mean maximal extent of individual snow grains

120   were measured in a woodland clearing. An artificial ice layer was created on the surface of the snowpack and compared with naturally formed ice layers. Artificial ice layers have been created in previous work (Montpetit et al., 2012) so it is important to know if their characteristics differ from naturally occurring ice layers. To create the ice layer a very thin top layer of undulating recent snow (less than 6 h old) was swept from the snowpack to expose a melt crust below, this was done

125   to maintain an ice layer of even thickness across the site. After the removal of recent snow, water was sprayed onto the snowpack to create a surface ice layer ~~(air temperatures were approximately −20C)~~ the ice layer was distinct to the melt-freeze crust and was removed from it when the layer was extracted. A natural ice layer covering the entire clearing was also present lower within the snowpack (formed by $2\,\mathrm{mm}$ of rain on 30 January). Density, bubble diameter, and thickness measurements

130   of both natural and artificial ice layers were made; whenever bubbles were visible their diameters

were measured using a field microscope and snow grain card, at a resolution of 0.1 mm. Very small bubbles, with a diameter of < 0.1 mm were recorded as being visible although a diameter could not be applied to them. Layer thickness was measured to a resolution of 1 mm for each sample. Density measurements were made of 15 natural and 15 of the artificial ice layer samples.

135   At CARE, measurements were conducted in an open, grass-covered field. A spatially continuous ice layer formed over an area of at least 200×100 m in the 10 cm deep snowpack as a result of above-freezing daytime temperatures for a period of 4 days prior to measurement. Ice layer thickness and densities were measured in the same manner as in North Bay, 29 measurements of ice density and thickness were made.

140   In Inuvik, water was sprayed onto a 30 cm tundra snowpack when air temperatures were approximately $-25\,°C$ to form an artificial ice layer on the surface of the snowpack as no natural ice layer was present. Water was sprayed over an area of 1 m^2, concentrating the spraying towards one edge, creating ~~an ice thickness gradient that~~ ice thicknesses between 1 and 6 mm which allowed 28 measurements of ice layer density across a ~~~~ range of ice layer thicknesses.

3   Results

3.1   Ice layer density

Mass and volume measurements were made of 86 samples of ice layers and are summarised in Table 2 and Fig. 3. After measurements were corrected for bias the mean sample volume was 6.4 cm^3 ~~meaning~~ when the random error ~~on the density measurements was~~ of $\pm$~~180~~.18 cm^3 was applied
150   to the volume measurements an uncertainty of ± 28 kg m^{-3} was calculated. Ice layer densities varied between 841 and 980 kg m^{-3}, with an overall mean of 909 kg m^{-3} and standard deviation of 23 kg m^{-3}, analysis using the Kolmogorov-Smirnov test showed all ice layers to be significantly different. Natural ice layers were on average less dense than artificial ones although the difference was within the methodological error. The measurements in Inuvik were made outside, and whilst
155   care was taken to ensure the balance was level and condensation was cleaned from the balance as it formed, these cannot be ruled out as sources of error and could be a reason why ~~the measured densities appear to be higher than is physically reasonable~~ some of the high outlying measured densities (3) are physically unreasonable at the Inuvik site. The air temperature was so cold that the water source for creating the artificial layers was freezing up, therefore it is considered unlikely that
160   the artificial ice layers were wet when measured.

3.2   Ice layer bubble size and thickness

Table 3 summarises the measurement of ice layer thickness and bubble size. In some cases bubbles were visible in the ice layer, but were not large enough to be measured using the field microscope. These were noted as < 0.1 mm in Table 3. For the purpose of calculating the mean and standard

165   deviation of the bubble distribution a value of 0.05 mm was applied to these bubbles. There was no significant correlation between ice layer thickness and bubble diameter ($p < 0.01$).

3.3 Error analysis

Three sources of error were quantified in the measurement of ice layer density: (1) systematic and (2) random error in the volumetric measurement of the ice samples, which would apply to any object

170   measured using this method (both discussed in Sect. 2.2), as well as (3) error from sample porosity, which applies only to the measurement of ice layer density. The measured ice layers had a closed porosity, where layers contained bubbles they were not connected in a porous structure. However, due to the presence of bubbles in the ice layers some increase in porosity would occur as more bubbles are exposed when the ice layer was broken and placed in the centrifuge tube~~, this is called~~

175   ~~the effective porosity~~. The exposure of the bubbles causes effective porosity and is represented by a dimensionless decimal fraction which represents the proportion of a volume which is available for liquid to flow through.

    The influence of effective porosity on the ice layer density measurements was quantitatively evaluated by numerically modelling the bubbles within ice layers. ~~Air~~ Air bubbles within the ice layer

180   were represented using spheres, scattered randomly without any overlap, within an ice sample of size x, y, z and density d. ~~Spheres were randomly placed within the x, y, z co-ordinate system without any overlap.~~ The sizes of the spheres were determined by taking a random sample from a normal distribution of bubble sizes based on the mean and standard deviation of bubble diameter measurements. A sphere size was chosen ~~from the random sample~~ randomly from the distribution and located ran-

185   domly within the x, y, z axes. If the sphere overlapped another sphere then the location was changed until no overlap occurred. If after 1000 attempts a location for the sphere could not be found its radius was changed to another random sample from the normal distribution and the process repeated. After each sphere was placed, the total volume of all the spheres and the density of the ice sample was calculated. Spheres were added to the sample until the desired density was reached starting from

190   an initial pure ice density of $916 \, \mathrm{kg\,m^{-3}}$. Examples of the ice layers with bubbles distributed in them are shown in Fig. 4.

    Slices were taken through the modelled ice sample and the volume of the spheres that would be open to the surface and allow liquid to penetrate the ice surface was calculated. For example, if the slice went through a sphere at exactly the halfway point, half of the volume of that sphere would be

195   added to the porosity value for that sample (Fig. 5). This method assumes that the ice layer is a solid ice layer containing bubbles rather than a granular snow-like structure. For a theoretical ice sample of size $10 \, \mathrm{mm} \times 10 \, \mathrm{mm} \times 10 \, \mathrm{mm}$ the sample density was increased in increments of $0.01 \, \mathrm{kg\,m^{-3}}$ from 600 to $916 \, \mathrm{kg\,m^{-3}}$, and porosity was measured through the sample by taking slices at $0.1 \, \mathrm{cm}$ intervals. The relationship between effective porosity and density (ρ) for this bubble and sample size

is linear and shown in Fig. 6, and the effective porosity (ϕ) ~~in~~ is found using:

$$\phi = -0.00016\rho + 0.14 \tag{1}$$

assuming the same porosity on all edges of the ice sample (where the sample was broken). The bubble diameter mean and standard deviation were taken as the overall values from all samples. The root-mean-squared-error of Eq. (1) was 0.0007 with an r squared value of 0.998.

The impact of this porosity on the samples was calculated by assuming a sample width of $2\,\mathrm{cm}$ (the width of the centrifuge tube). Sample thickness and volume were measured (with known methodological error) and used to estimate the maximum and minimum dimensions of each sample. The relationship in Eq. (1) was used to estimate the porosity of each sample based on the measured density. ~~Sample porosities~~ As the density of the sample decreased volume error from porosity in the sample ranged from 6.5×10^{-5} to ~~0.001~~ $1 \times 10^{-3}\,\mathrm{cm}^3$. The mean increase using either the maximum or minimum value for density in the porosity calculations was $1.42 \times 10^{-6}\,\mathrm{cm}^3$. The maximum random error ($\pm 0.18\,\mathrm{cm}^3$), the volume measurement bias reflecting systematic error ($-0.19\,\mathrm{cm}^3$), and the porosity correction were applied to each volume measurement and the maximum range of density was calculated for each sample, the samples' porosity was negligible (less than $0.001\,\mathrm{cm}^3$). Overall the measurements of ice layer density (~~909 ± 18~~ $909 \pm 28\,\mathrm{kg\,m}^{-3}$) were not significantly different to the actual density of pure ice (Table 1).

4   Discussion and conclusion

New laboratory and field protocols were used to produce direct measurements of ice layer density including a thorough assessment of measurement uncertainty. Measurements of natural and artificially made ice layers produced an average density of ~~909 ± 18~~ $909 \pm 28\,\mathrm{kg\,m}^{-3}$, where uncertainty is a function of the random error in the method used to measure the volume of the ice samples. Effective porosity of ice layers was estimated using observations of bubble size and was deemed to be too low to impact the accuracy of the method. Our measured density values are higher than those previously measured by Marsh (1984) (mean $800\,\mathrm{kg\,m}^{-3}$), and Pfeffer and Humphrey (1996) (400 to $800\,\mathrm{kg\,m}^{-3}$). It is unclear whether previous studies measured the density of ice layers that were permeable and porous, including thin, non-continuous ice layers. Here only impermeable ice layers were measured and this may explain the density differences between studies.

Artificially created ice layers had a higher density than natural ice layers (Table 2), a possible reason for this is that the artificial ice layers were created on the surface of the snowpack, and in low air temperatures. This means that they are likely to be colder than the naturally formed ice layers, which were found in the middle of the snowpack. Because ice density increases as temperatures decrease (Table 1) this could account for the higher densities. For this reason it is recommended that for the purposes of snow emission modelling, only the density measurements from the natural ice layers are used. Further work is required to characterise the structural differences between natural

235 and artificial ice layers, in order to determine if artificial and natural ice layers have the same radiative transfer properties.

Impermeable ice layer microstructure consists of a layer of ice containing small bubbles. Successive melt-refreeze events cause densification of a snow layer which forms an ice crust and eventually
240 an impermeable ice layer (Fierz et al., 2009). Densification and ice formation impacts passive microwave brightness temperatures at the satellite scale (Grody, 2008), therefore the evolution of ice structures is important in characterisation of snowpack microwave signatures, and may play an important role in ice layer detection algorithms. Snow microwave emission models are currently unable to accurately model ice layers (Rees et al., 2010). Some snow emission models e.g. Wiesmann and Mätzler (1999); Picard et al. (2013) include a parameter for ice layer density, which has previously
245 been unknown and is potentially a large source of error (Durand et al., 2008). Ice layers form an important part of runoff modelling, where impermeable and high density ice layers form barriers or redirect runoff in a stratified snowpack (Langham, 1974; Marsh, 1984; Katsushima et al., 2009). The accuracy of the representation of ice layers in snow models is important in both runoff modelling (Hirashima et al., 2010), and remote sensing data assimilation applications (Langlois et al.,
250 2012) and without accurate ice layer density data, our ability to simulate snowpacks is not known. To further quantify the density of ice layers, an intercomparison of different methods of measuring ice layer density, and collection of reference measurements using a gas pycnometer or similar device, would help provide certainty and context to all the previous measurements. Ideally this data would be collected in a variety of snow types and the applicability of these density measurements
255 to ice lenses in addition to ice layers could be assessed. Measuring the density of ice crusts, which are also a challenge for microwave modelling (Pan et al., 2014), would require a different method of measurement as ice crusts are permeable.

As the earth's climate warms, melt-refreeze and rain-on-snow events are predicted to become increasingly common (Freudiger et al., 2014; Ye et al., 2008). In order to accurately quantify the
260 change, and predict the impact of these events on the Arctic and mid-latitudes, it is necessary that ice layers are accurately accounted for in modelled and observed land surface and snow data products. Density is a fundamental parameter in the description of ice and snow microstructure (Mätzler, 2002), which will benefit from improved measurement accuracy and constrained uncertainty using techniques outlined in this study.

270   References

Albert, M. R. and Perron Jr., F. E.: Ice layer and surface crust permeability in a seasonal snowpack, Hydrol. Process., 14, 3207–3214, 2000.

Colbeck, S. C.: The layered character of snow covers, Rev. Geophys., 29, 81–96, 1991.

Colbeck, S. C. and Anderson, E. A.: The permiability of melting snow, Water Resour. Res., 18, 904–908, 1982.

275   Durand, M. T., Kim, E. J., and Margulis, S. A.: Quantifying uncertainty in modeling snow microwave radiance for a mountain snowpack at the point-scale, including stratigraphic effects, IEEE T. Geosci. Remote, 46, 1753–1767, 2008.

Eisenberg, D. S. and Kauzmann, W.: The Structure and Properties of Water, Oxford University Press, Oxford, 1969.

280   Fierz, C., Armstrong, R. L., Durand, Y., Etchevers, P., Greene, E., McClung, D. M., Nishimura, K., Satyawali, P. K., and Sokratov, S. A.: The international classification for seasonal snow on the ground, UNESCO/IHP, Paris, 2009.

Freudiger, D., Kohn, I., Stahl, K., and Weiler, M.: Large-scale analysis of changing frequencies of rain-on-snow events with flood-generation potential, Hydrol. Earth Syst. Sci., 18, 2695–2709, doi:10.5194/hess-18-2695-2014, 2014.

285   Gray, D. M. and Male, D. H.: Handbook of Snow, The Blackburn Press, Caldwell, New Jersey, 1981.

Grenfell, T. C. and Putkonen, J.: A method for the detection of the severe rain-on-snow event on Banks Island, October 2003, using passive microwave remote sensing, Water Resour. Res., 44, W03425, doi:10.1029/2007WR005929, 2008.

290   Grody, N.: Relationship between snow parameters and microwave satellite measurements: Theory compared with advanced microwave sounding unit observations from 23 to 150 GHz, J. Geophys. Res.-Atmos., 113, 1–17, 2008.

Hirashima, H., Yamaguchi, S., Sato, A., and Lehning, M.: Numerical modeling of liquid water movement through layered snow based on new measurements of the water retention curve, Cold Reg. Sci. Technol., 64, 295   94–103, 2010.

Hobbs, P. V.: Ice Physics, Clarendon Press, Oxford, UK, 1974.

Katsushima, T., Kumakura, T., and Takeuchi, Y.: A multiple snow layer model including a parameterization of vertical water channel process in snowpack, Cold Reg. Sci. Technol., 59, 143–151, 2009.

Keegan, K., Albert, M. R., and Baker, I.: The impact of ice layers on gas transport through firn at the North 300   Greenland Eemian Ice Drilling (NEEM) site, Greenland, The Cryosphere, 8, 1801–1806, doi:10.5194/tc-8-1801-2014, 2014.

Kumpula, J., Parikka, P., and Nieminen, M.: Occurrence of certain microfungi on reindeer pastures in northern Finland during winter 1996–97, Rangifer, 20, 3–8, 2000.

La Placa, S. J. and Post, B.: Thermal expansion of ice, Acta Crystallogr., 13, 503–505, 1960.

305   Langham, E. J.: Phase equilibria of veins in polycrystalline ice, Can. J. Earth Sci., 11, 1280–1287, 1974.

Langlois, A., Royer, A., Derksen, C., Montpetit, B., Dupont, F., and Goïta, K.: Coupling of the snow thermodynamic model SNOWPACK with the Microwave Emission Model for Layered Snowpacks (MEMLS) for subarctic and arctic snow water equivalent retrievals, Water Resour. Res., 48, 819–821, doi:10.1029/2012WR012133, 2012.

310 Lemmetyinen, J., Pulliainen, J., Rees, A., Kontu, A., and Derksen, C.: Multiple-layer adaptation of HUT Snow Emission Model: comparison with experimental data, IEEE T. Geosci. Remote, 48, 2781–2794, 2010.

Lonsdale, D. K.: The structure of ice, P. Roy. Soc. Lond. A Mat., 247, 424–434, 1958.

Marsh, P.: Wetting front advance and freezing of meltwater within a snow cover: 1. Observations in the Canadian Arctic, Water Resour. Res., 20, 1853–1864, 1984.

315 Mätzler, C.: Relation between grain-size and correlation length of snow, J. Glaciol., 48, 461–466, 2002.

Mätzler, C. and Wiesmann, A.: Extension of the microwave emission model of layered snowpacks to coarse-grained snow, Remote Sens. Environ., 325, 317–325, 1999.

Montpetit, B., Royer, A., Roy, A., Langlois, A., and Derksen, C.: Snow microwave emission modeling of ice lenses within a snowpack using the microwave emission model for layered snowpacks, IEEE T. Geosci.

320 Remote, 51, 4705–4717, 2012.

Pan, J., Jiang, L., and Zhang, L.: Comparison of the multi-layer HUT snow emission model with observations of wet snowpacks, Hydrol. Process., 28, 1071–1083, 2014.

Pfeffer, W. T. and Humphrey, N. F.: Determination of timing and location of water movement and ice-layer formation by temperature measurements in sub-freezing snow, J. Glaciol., 42, 292–304, 1996.

325 Picard, G., Brucker, L., Roy, A., Dupont, F., Fily, M., Royer, A., and Harlow, C.: Simulation of the microwave emission of multi-layered snowpacks using the Dense Media Radiative transfer theory: the DMRT-ML model, Geosci. Model Dev., 6, 1061–1078, doi:10.5194/gmd-6-1061-2013, 2013.

Putkonen, J. and Roe, G.: Rain-on-snow events impact soil temperatures and affect ungulate survival, Geophys. Res. Lett., 30, 37, doi:10.1029/2002GL016326, 2003.

330 Rees, A., Lemmetyinen, J., Derksen, C., Pulliainen, J., and English, M.: Observed and modelled effects of ice lens formation on passive microwave brightness temperatures over snow covered tundra, Remote Sens. Environ., 114, 116–126, 2010.

Sihvola, A. and Tiuri, M.: Snow fork for field determination of the density and wetness profiles of a snow pack, IEEE T. Geosci. Remote, GE-24, 717–721, 1986.

335 Takala, M., Luojus, K., Pulliainen, J., Derksen, C., Lemmetyinen, J., Kärnä, J.-P., Koskinen, J. T., and Bojkov, B.: Estimating northern hemisphere snow water equivalent for climate research through assimilation of space-borne radiometer data and ground-based measurements, Remote Sens. Environ., 115, 3517–3529, 2011.

Wiesmann, A. and Mätzler, C.: Microwave emission model of layered snowpacks, Remote Sens. Environ., 70,

340 307–316, 1999.

Ye, H., Yang, D., and Robinson, D.: Winter rain on snow and its association with air temperature in northern Eurasia, Hydrol. Process., 22, 2728–2736, 2008.

Table 1. Measurements of pure ice density, adapted from Hobbs (1974).

Temperature (°C)	Density (kg m^{-3})	Reference
0	916.4	Lonsdale (1958) using diffraction measurements
−30	919.3	
−60	922.7	
−10	918.7	Eisenberg and Kauzmann (1969)
−20	920.3	based on X-ray diffraction measurements
−40	922.8	made by La Placa and Post (1960)

Table 2. Ice layer density measurements, (all values have been corrected to account for the measured $-0.19\,\text{cm}^3$ bias in volume).

Site	n	Mean (kg m^{-3})	SD (kg m^{-3})
CARE – Natural	29	906	17
North Bay – Natural	15	890	21
North Bay – Artificial	15	921	18
Inuvik – Artificial	28	915	26

Table 3. Measurements of ice layer bubble size and ice layer thickness (all sizes in mm). n is number of samples, $n < 0.1$ is the number of bubbles with diameter of less than 0.1 mm.

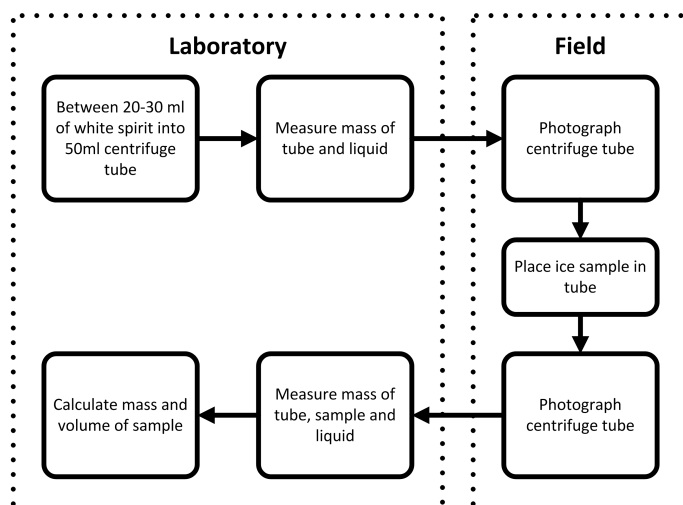|			Bubble Diameter				Layer Thickness	
	Type	n	$n < 0.1$	Mean	SD	n	Mean	SD
CARE	Natural	0	–	–	–	29	8	0.6
North Bay	Natural	14	4	0.16	0.12	15	3	0.6
	Artificial	12	6	0.08	0.03	15	5	0.9
Inuvik	Artificial	0	–	–	–	28	2	0.5
Overall	–		26	10	0.12	0.1	86	5	2.7

Figure 1. Flow chart describing the methodology to measure densities of ice layers from a snowpack.
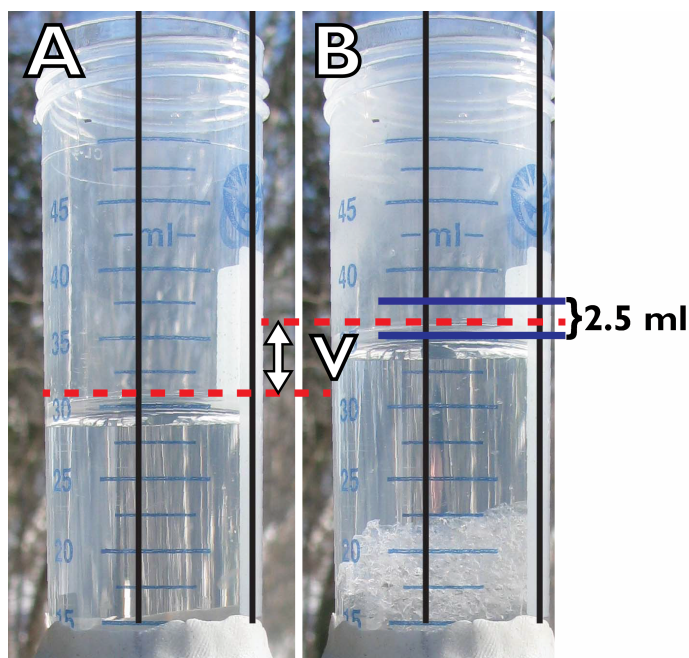

Figure 2. Example of pair of photos used in calculation of ice sample volume. **(a)** taken before the sample was added and **(b)**, taken after. V is equal to the volume of the ice sample. Black lines are guides added to help assess the quality of the photos.
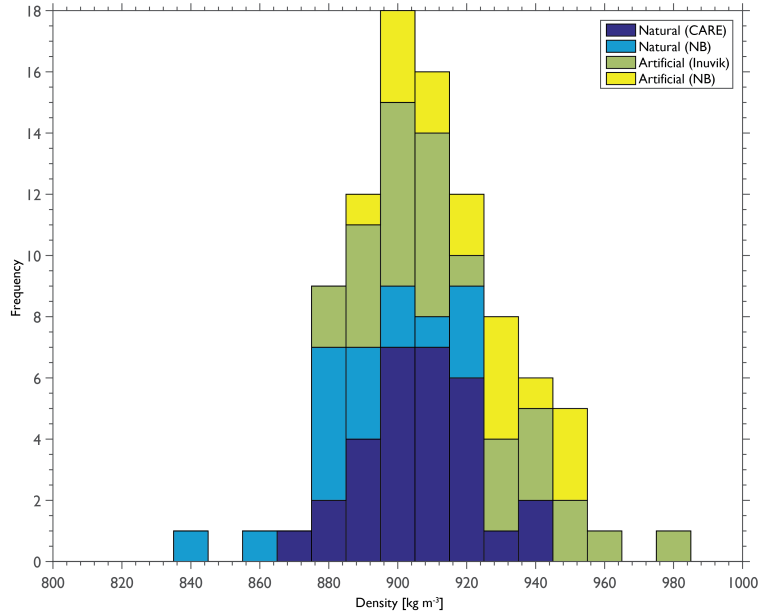
Figure 3. Summary of ice layer density measurements. Stacked histogram showing frequency of each density measurement, colours show distribution of artificial and natural ice layers across multiple sites.

Figure 4. Examples of the numerical representation of ice layers used to investigate porosity, **(a)** shows a sample with simulated density of $800 \, \text{kg} \, \text{m}^{-3}$ and **(b)** shows a sample with density $909 \, \text{kg} \, \text{m}^{-3}$.
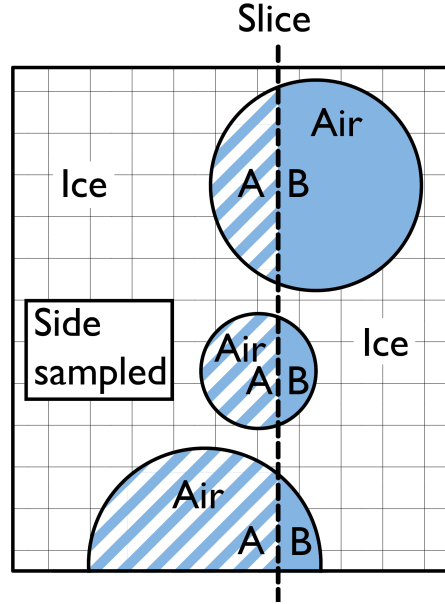
Figure 5. Schematic representation of slicing technique to measure porosity. Air bubbles (shaded in blue) are shown in an ice sample, the theoretical slice was made at the location of the dashed line. The left hand side was chosen as the side to be sampled, and so all of the diagonally striped areas marked "A" were calculated and summed to calculate the overall porosity of the sample.
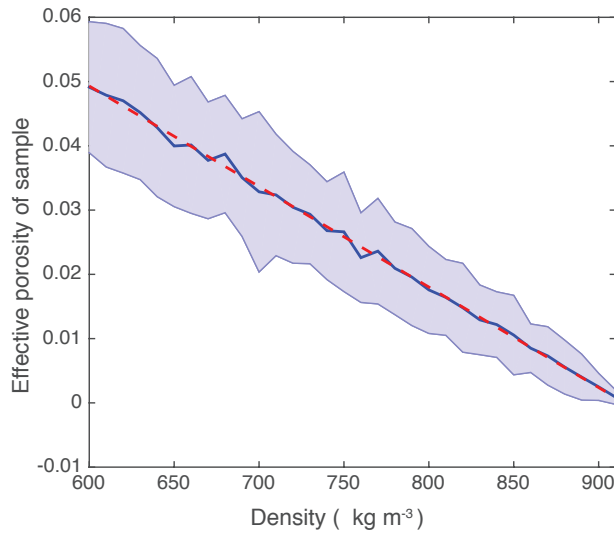

Figure 6. ~~The effect of~~ Sample density ~~on the~~ vs mean simulated sample porosity (Blue line). Sample porosity was calculated at $0.1\,\mathrm{cm}$ intervals throughout the sample, shaded area shows mean ± 1 standard deviation. Red dashed fitted linear trend line (Eq. 1) was calculated using a least squares regression.

Improved measurement of ice layer density in seasonal snowpacks

T. Watts[1], N. Rutter[1], P. Toose[2], C. Derksen[2], M. Sandells[3,a], and J. Woodward[1]

[1]Department of Geography, Northumbria University, Newcastle upon Tyne, NE1 8ST, UK
[2]Climate Research Division, Environment Canada, Toronto, Canada
[3]National Centre for Earth Observation, University of Reading, Reading, RG6 6AL, UK
[a]now at: CORES Science and Engineering Limited, Victoria Garesfield, UK

Correspondence to: N. Rutter (nick.rutter@northumbria.ac.uk)

Abstract. Ice layers in snowpacks introduce uncertainty in satellite derived estimates of snow water equivalent, have ecological impacts on plants and animals, and change the thermal and vapour transport properties of the snowpack. The microstructure and specifically the density of ice layers is poorly quantified. Here we present a new field method, for measuring the density of ice layers caused by melt or rain-on-snow events. The method was used on 87 ice layer samples in the Canadian Arctic and mid-latitudes; the mean measured ice layer density was $909 \pm 28\,\mathrm{kg\,m^{-3}}$ with a standard deviation of $23\,\mathrm{kg\,m^{-3}}$, significantly higher than values typically used in the literature.

1 Introduction

Ice structures form in snowpacks during melt or rain-on-snow events (Colbeck, 1991). Rain either freezes on contact with the surface of the snowpack, or water refreezes within the snowpack to form ice layers, lenses, crusts, columns, or basal ice layers (Gray and Male, 1981). Strong intercrystalline bonds created from refreezing of liquid water, lead to the formation of cohesive ice structures (Fierz et al., 2009). The presence of ice layers changes the thermal and vapour transport properties of the snowpack, which increases soil temperature (Putkonen and Roe, 2003), and encourages the growth of fungus and molds that lead ungulate deaths (Kumpula et al., 2000). Additionally the physical barrier to subnivean vegetation presented by ice layers in the snowpack is linked with a large reduction in ungulate survival via starvation and reduced calf production rate (Grenfell and Putkonen, 2008). Permeability of ice layers to liquid water and gas is vastly reduced compared to snow (Albert and Perron Jr., 2000; Colbeck and Anderson, 1982; Keegan et al., 2014). Impermeable layers are identifiable because pores do not connect within the ice formation, and the granular snowpack structure is missing (Fierz et al., 2009). Ice layers differ from ice crusts and ice lenses; ice crusts are always permeable and have a coarse grained granular snow-like structure (Colbeck and Anderson, 1982). Ice lenses can be impermeable, do not have a granular structure and are spatially discontinuous. Sim-

ilarly to ice lenses, ice layers can be impermeable, and do not have a granular structure, however, ice layers are continuous (Fierz et al., 2009).

Ice layers introduce uncertainty into the performance of snow microwave emission models (Rees et al., 2010), which are an important component of satellite derived snow water equivalent (SWE) retrieval algorithms (Takala et al., 2011). The radiometric influence of thin ice layers poses a significant challenge for physical and semi-empirical emission models, which can either treat ice layers as coarse grained snow (Mätzler and Wiesmann, 1999) or as planar (flat and smooth) ice layers (Lemmetyinen et al., 2010).

As the climate warms, an increase in the number of mid-season melt and rain-on-snow events is predicted (Putkonen and Roe, 2003), which will likely increase the occurrence of ice layers in the Arctic (Ye et al., 2008) and mid-latitudes (Freudiger et al., 2014). The microstructure and properties of ice layers remain poorly quantified with field observations, which hinders snow emission model development and evaluation (Montpetit et al., 2012). Durand et al. (2008) carried out sensitivity studies and simulations of mountain snowpack brightness temperature with the Microwave Emission Model of Layered Snowpacks (MEMLS) (Wiesmann and Mätzler, 1999). The lack of an accurate ice layer density measurement technique, meant that the uncertainties attributed to not knowing the density of ice layers were 32.2 and 15.3 K for horizontally polarised (H-pol) 18.7 and 36.5 GHz frequencies respectively, a greater uncertainty than any other parameter investigated (Durand et al., 2008).

Pure ice density ranges from $916 \, \mathrm{kg \, m^{-3}}$ at $0 \, °\mathrm{C}$ to $922 \, \mathrm{kg \, m^{-3}}$ at $-40 \, °\mathrm{C}$ (Table 1). Only limited field measurements of ice layer densities have previously been attempted. Ice layer density measurements taken in the Canadian Arctic by submerging pieces of ice crust into oil resulted in a range of densities from 630 to $950 \, \mathrm{kg \, m^{-3}}$ (Marsh, 1984). Ice layer densities of 400 to $800 \, \mathrm{kg \, m^{-3}}$ were measured using a snow fork (which measures the dielectric properties of snow around 1 GHz (Sihvola and Tiuri, 1986)) in seasonal snow on the Greenland ice sheet (Pfeffer and Humphrey, 1996). The results from these studies vary drastically and a quantitative assessment of the error in measurement techniques is absent. Consequently, the aim of this paper is to describe a newly developed field measurement technique for measuring ice layer density, and present density measurements made in Arctic and mid-latitude snowpacks.

2 Method

2.1 Development of ice density measurement method

A new laboratory and field-based method was developed to measure the density of ice layers found in seasonal snow, based on volumetric displacement. The basic principle is that when an ice layer sample is submerged in a vessel of liquid, calculating the volume displacement and sample mass will yield an estimate of density. The laboratory and field protocols for measuring the density of ice

layers with this method is outlined in Fig. 1. The mass of a sealed $50\,\mathrm{mL}$ centrifuge tube with $2.5\,\mathrm{mL}$ graduations containing white spirit (sometimes termed "mineral spirits"), was measured with a precision of $\pm0.001\,\mathrm{g}$ under laboratory conditions before entering the field. White spirit is immiscible with water and has a low freezing point ($-70\,^{\circ}\mathrm{C}$), eliminating potential sample melt. White spirit also has a low density ($650\,\mathrm{kg\,m^{-3}}$), making it likely that the ice sample would sink and be completely submerged. In the field the centrifuge tube was held by a fixed, levelled, mounting system within the macro setting range of a compact camera. Each camera image was centred on a visible datum on the mounting system to ensure the camera was correctly focused, and that repeat images were consistently made from the same horizontal position. Images were taken before and after each ice sample was submerged as shown in Fig. 2.

In each image three positions were identified during post processing: the liquid level, the graduation above the liquid level and the graduation below the liquid level. Pixel co-ordinates of these positions were recorded and the proportional height of the liquid level between the upper and lower graduation was translated to a volume at a higher resolution than the centrifuge tube graduations alone would allow. The top of the liquid level was located rather than the meniscus for ease of identification; as relative volume change was used no error was introduced. After images were taken, the centrifuge tube containing the sample was sealed and the change in mass was measured on return to the laboratory. Only samples where the liquid in the tube was level in both images were considered.

2.2 Methodological error

Ice layers found in snowpacks are very difficult to accurately and consistently re-create under laboratory conditions. Therefore to assess the accuracy of the ice density measurement technique, ball bearings of known volume were measured. Stainless steel ball bearings were used (manufactured to a diameter of $1\pm2.5\times10^{-5}\,\mathrm{cm}$), resulting in a volume of $0.5236\pm0.0004\,\mathrm{cm^3}$. The volume of the ball bearings was calculated from before and after images of 10 ball bearings submerged in the centrifuge tube. The expected total volume of all ball bearings of approximately $5.236\,\mathrm{cm^3}$ is comparable to the mean volume of ice samples collected. Of 134 samples, each consisting of 10 ball bearings, the mean volume was $5.045\,\mathrm{cm^3}$. The volume measurements were normally distributed and an error value based on ±1 standard deviations was calculated, resulting in a systematic volume measurement error or bias of $-0.19\,\mathrm{cm^3}$.

The largest source of error is in reading the height of the liquid in the centrifuge tube from the camera photos. Identifying the precise height of the surface of the liquid between the graduation markings on the cylinder is limited by the quality of the camera focus and resolution of the camera. If the camera focus is not perfect it is difficult to locate the height of the liquid, which result in error and uncertainty. Based on carrying out 10 repeat measurements on 10 centrifuge tube photos the (mean) error was found to be $\pm0.125\,\mathrm{cm^3}$ in each volume measurement photo, equating to a root mean squared

error in the measurement of the ice sample volume of $\pm 0.18\,\mathrm{cm}^3$ ($error = \sqrt{0.125^2 + 0.125^2}$), as each volume measurement involves reading the volume from two photos.

To calculate the optimum sample volume the number of ball bearings used in each volume measurement was increased from 1 to 24, a volume range of 0.52 to $12.57\,\mathrm{cm}^3$. Correlation between standard deviation and sample volume was not statistically significant (confidence > 99 %), demonstrating that the error in volume measurement was independent of sample volume. Field trials suggested that $10\,\mathrm{cm}^3$ was the maximum sample volume routinely possible to use due to the diameter of the centrifuge tube. Although no minimum sample volume was set, the largest possible sample was obtained.

To estimate the potential impact of the uncertainty in volume measurement on samples taken in the field, the random ($\pm 0.18\,\mathrm{cm}^3$) volume measurement error from the ball bearing experiment was applied to a theoretical ice sample of volume $4.89\,\mathrm{cm}^3$ and mass 4.53 g (equating to a density of $916\,\mathrm{kg\,m}^{-3}$). This volume error from the ball bearing experiment translated into an observed volume of 4.53–$4.89\,\mathrm{cm}^3$ (i.e. $4.71 \pm 0.18\,\mathrm{cm}^3$). Assuming no error in the mass balance (precision of ± 0.001 g), the upper density value (minimum volume) was $951\,\mathrm{kg\,m}^{-3}$ and the lower density value (maximum volume) was $881\,\mathrm{kg\,m}^{-3}$, representing an uncertainty in density of $\pm 35\,\mathrm{kg\,m}^{-3}$ or 4 %.

2.3 Field measurements

During the winter of 2013, ice layer density measurements were collected at three sites in Canada: North Bay, Ontario (46.33° N, 79.31° W) between 8–9 February, Canadian Centre for Atmospheric Research (CARE), Egbert, Ontario (44.23° N, 79.78° W) on 25 February, and Trail Valley Creek, Inuvik, North West Territories (68.72° N, 133.16° W) on 9 April. Ice layers were removed from the surrounding snow and broken to size using a scraper.

In North Bay, snow stratigraphy, density and the mean maximal extent of individual snow grains were measured in a woodland clearing. An artificial ice layer was created on the surface of the snowpack and compared with naturally formed ice layers. Artificial ice layers have been created in previous work (Montpetit et al., 2012) so it is important to know if their characteristics differ from naturally occurring ice layers. To create the ice layer a very thin top layer of undulating recent snow (less than 6 h old) was swept from the snowpack to expose a melt crust below, this was done to maintain an ice layer of even thickness across the site. After the removal of recent snow, water was sprayed onto the snowpack to create a surface ice layer. The ice layer was distinct to the melt-freeze crust and was removed when the layer was extracted. A natural ice layer covering the entire clearing was also present lower within the snowpack (formed by 2 mm of rain on 30 January). Density, bubble diameter, and thickness measurements of both natural and artificial ice layers were made; whenever bubbles were visible their diameters were measured using a field microscope and snow grain card, at a resolution of 0.1 mm. Very small bubbles, with a diameter of < 0.1 mm were

130 recorded as being visible although a diameter could not be applied to them. Layer thickness was measured to a resolution of 1 mm for each sample. Density measurements were made of 15 natural and 15 of the artificial ice layer samples.

At CARE, measurements were conducted in an open, grass-covered field. A spatially continuous ice layer formed over an area of at least 200×100 m in the 10 cm deep snowpack as a result of above-

135 freezing daytime temperatures for a period of 4 days prior to measurement. Ice layer thickness and densities were measured in the same manner as in North Bay, 29 measurements of ice density and thickness were made.

In Inuvik, water was sprayed onto a 30 cm tundra snowpack when air temperatures were approximately $-25\,^{\circ}$C to form an artificial ice layer on the surface of the snowpack as no natural ice layer

140 was present. Water was sprayed over an area of 1 m^2, concentrating the spraying towards one edge, creating ice thicknesses between 1 and 6 mm which allowed 28 measurements of ice layer density across a range of ice layer thicknesses.

3 Results

3.1 Ice layer density

145 Mass and volume measurements were made of 86 samples of ice layers and are summarised in Table 2 and Fig. 3. After measurements were corrected for bias the mean sample volume was 6.4 cm^3 when the random error of ± 0.18 cm^3 was applied to the volume measurements an uncertainty of ± 28 kg m^{-3} was calculated. Ice layer densities varied between 841 and 980 kg m^{-3}, with an overall mean of 909 kg m^{-3} and standard deviation of 23 kg m^{-3}. Analysis using the Kolmogorov-Smirnov

150 test showed all ice layers to be significantly different to all other ice layers. Natural ice layers were on average less dense than artificial ones although the difference was within the methodological error. The measurements in Inuvik were made outside, and whilst care was taken to ensure the balance was level and condensation was cleaned from the balance as it formed, these cannot be ruled out as sources of error and could be a reason why some of the high outlying measured densities (Figure 3)

155 are physically unreasonable at the Inuvik site. The air temperature was so cold that the water source for creating the artificial layers was freezing up, therefore it is considered unlikely that the artificial ice layers were wet when measured.

3.2 Ice layer bubble size and thickness

Table 3 summarises the measurement of ice layer thickness and bubble size. In some cases bubbles

160 were visible in the ice layer, but were not large enough to be measured using the field microscope. These were noted as < 0.1 mm in Table 3. For the purpose of calculating the mean and standard deviation of the bubble distribution a value of 0.05 mm was applied to these bubbles. There was no significant correlation between ice layer thickness and bubble diameter ($p < 0.01$).

3.3 Error analysis

165 Three sources of error were quantified in the measurement of ice layer density: (1) systematic and (2) random error in the volumetric measurement of the ice samples, which would apply to any object measured using this method (both discussed in Sect. 2.2), as well as (3) error from sample porosity, which applies only to the measurement of ice layer density. The measured ice layers had a closed porosity, where layers contained bubbles they were not connected in a porous structure. However,

170 due to the presence of bubbles in the ice layers some increase in porosity would occur as more bubbles are exposed when the ice layer was broken and placed in the centrifuge tube. The exposure of the bubbles causes effective porosity and is represented by a dimensionless decimal fraction which represents the proportion of a volume which is available for liquid to flow through.

The influence of effective porosity on the ice layer density measurements was quantitatively eval-

175 uated by numerically modelling the bubbles within ice layers. Air bubbles within the ice layer were represented using spheres, scattered randomly without any overlap, within an ice sample of size x, y, z and density d. The sizes of the spheres were determined by taking a random sample from a normal distribution of bubble sizes based on the mean and standard deviation of bubble diameter measurements. A sphere size was chosen randomly from the distribution and located randomly

180 within the x, y, z axes. If the sphere overlapped another sphere then the location was changed until no overlap occurred. If after 1000 attempts a location for the sphere could not be found its radius was changed to another random sample from the normal distribution and the process repeated. After each sphere was placed, the total volume of all the spheres and the density of the ice sample was calculated. Spheres were added to the sample until the desired density was reached starting from an

185 initial pure ice density of 916 kg m^{-3}. Examples of the ice layers with bubbles distributed in them are shown in Fig. 4.

Slices were taken through the modelled ice sample and the volume of the spheres that would be open to the surface and allow liquid to penetrate the ice surface was calculated. For example, if the slice went through a sphere at exactly the halfway point, half of the volume of that sphere would be

190 added to the porosity value for that sample (Fig. 5). This method assumes that the ice layer is a solid ice layer containing bubbles rather than a granular snow-like structure. For a theoretical ice sample of size $10\,\mathrm{mm} \times 10\,\mathrm{mm} \times 10\,\mathrm{mm}$ the sample density was increased in increments of $0.01\,\mathrm{kg\,m}^{-3}$ from 600 to $916\,\mathrm{kg\,m}^{-3}$, and porosity was measured through the sample by taking slices at $0.1\,\mathrm{cm}$ intervals. The relationship between effective porosity and density (ρ) for this bubble and sample size

195 is linear and shown in Fig. 6, and the effective porosity (ϕ) is found using:

$$\phi = -0.00016\rho + 0.14 \tag{1}$$

assuming the same porosity on all edges of the ice sample (where the sample was broken). The bubble diameter mean and standard deviation were taken as the overall values from all samples. The root-mean-squared-error of Eq. (1) was 0.0007 with an r squared value of 0.998.

200   The impact of this porosity on the samples was calculated by assuming a sample width of $2\,\mathrm{cm}$ (the width of the centrifuge tube). Sample thickness and volume were measured (with known methodological error) and used to estimate the maximum and minimum dimensions of each sample. The relationship in Eq. (1) was used to estimate the porosity of each sample based on the measured density. As the density of the sample decreased, volume error from porosity in the sample ranged from

205   6.5×10^{-5} to $1 \times 10^{-3}\,\mathrm{cm^3}$. The mean increase using either the maximum or minimum value for density in the porosity calculations was $1.42 \times 10^{-6}\,\mathrm{cm^3}$. The maximum random error ($\pm 0.18\,\mathrm{cm^3}$), the volume measurement bias reflecting systematic error ($-0.19\,\mathrm{cm^3}$), and the porosity correction were applied to each volume measurement and the maximum range of density was calculated for each sample, the samples' porosity was negligible (less than $0.001\,\mathrm{cm^3}$). Overall the measurements

210   of ice layer density ($909 \pm 28\,\mathrm{kg\,m^{-3}}$) were not significantly different to the actual density of pure ice (Table 1).

4 Discussion and conclusion

New laboratory and field protocols were used to produce direct measurements of ice layer density including a thorough assessment of measurement uncertainty. Measurements of natural and artificially

215   made ice layers produced an average density of $909 \pm 28\,\mathrm{kg\,m^{-3}}$, where uncertainty is a function of the random error in the method used to measure the volume of the ice samples. Effective porosity of ice layers was estimated using observations of bubble size and was deemed to be too low to impact the accuracy of the method. Our measured density values are higher than those previously measured by Marsh (1984) (mean $800\,\mathrm{kg\,m^{-3}}$), and Pfeffer and Humphrey (1996) (400 to $800\,\mathrm{kg\,m^{-3}}$). It is

220   unclear whether previous studies measured the density of ice layers that were permeable and porous, including thin, non-continuous ice layers. Here only impermeable ice layers were measured and this may explain the density differences between studies.

Artificially created ice layers had a higher density than natural ice layers (Table 2), a possible reason for this is that the artificial ice layers were created on the surface of the snowpack, and in low

225   air temperatures. This means that they are likely to be colder than the naturally formed ice layers, which were found in the middle of the snowpack. Because ice density increases as temperatures decrease (Table 1) this could account for the higher densities. For this reason it is recommended that for the purposes of snow emission modelling, only the density measurements from the natural ice layers are used. Further work is required to characterise the structural differences between natural

230   and artificial ice layers, in order to determine if artificial and natural ice layers have the same radiative transfer properties.

Impermeable ice layer microstructure consists of a layer of ice containing small bubbles. Successive melt-refreeze events cause densification of a snow layer which forms an ice crust and eventually an impermeable ice layer (Fierz et al., 2009). Densification and ice formation impacts passive mi-

7

crowave brightness temperatures at the satellite scale (Grody, 2008), therefore the evolution of ice structures is important in characterisation of snowpack microwave signatures, and may play an important role in ice layer detection algorithms. Snow microwave emission models are currently unable to accurately model ice layers (Rees et al., 2010). Some snow emission models e.g. Wiesmann and Mätzler (1999); Picard et al. (2013) include a parameter for ice layer density, which has previously been unknown and is potentially a large source of error (Durand et al., 2008). Ice layers form an important part of runoff modelling, where impermeable and high density ice layers form barriers or redirect runoff in a stratified snowpack (Langham, 1974; Marsh, 1984; Katsushima et al., 2009). The accuracy of the representation of ice layers in snow models is important in both runoff modelling (Hirashima et al., 2010), and remote sensing data assimilation applications (Langlois et al., 2012) and without accurate ice layer density data, our ability to simulate snowpacks is not known. To further quantify the density of ice layers, an intercomparison of different methods of measuring ice layer density, and collection of reference measurements using a gas pycnometer or similar device, would help provide certainty and context to all the previous measurements. Ideally this data would be collected in a variety of snow types and the applicability of these density measurements to ice lenses in addition to ice layers could be assessed. Measuring the density of ice crusts, which are also a challenge for microwave modelling (Pan et al., 2014), would require a different method of measurement as ice crusts are permeable.

As the earth's climate warms, melt-refreeze and rain-on-snow events are predicted to become increasingly common (Freudiger et al., 2014; Ye et al., 2008). In order to accurately quantify the change, and predict the impact of these events on the Arctic and mid-latitudes, it is necessary that ice layers are accurately accounted for in modelled and observed land surface and snow data products. Density is a fundamental parameter in the description of ice and snow microstructure (Mätzler, 2002), which will benefit from improved measurement accuracy and constrained uncertainty using techniques outlined in this study.

265 **References**

Albert, M. R. and Perron Jr., F. E.: Ice layer and surface crust permeability in a seasonal snowpack, Hydrol. Process., 14, 3207–3214, 2000.

Colbeck, S. C.: The layered character of snow covers, Rev. Geophys., 29, 81–96, 1991.

Colbeck, S. C. and Anderson, E. A.: The permiability of melting snow, Water Resour. Res., 18, 904–908, 1982.

270 Durand, M. T., Kim, E. J., and Margulis, S. A.: Quantifying uncertainty in modeling snow microwave radiance for a mountain snowpack at the point-scale, including stratigraphic effects, IEEE T. Geosci. Remote, 46, 1753–1767, 2008.

Eisenberg, D. S. and Kauzmann, W.: The Structure and Properties of Water, Oxford University Press, Oxford, 1969.

275 Fierz, C., Armstrong, R. L., Durand, Y., Etchevers, P., Greene, E., McClung, D. M., Nishimura, K., Satyawali, P. K., and Sokratov, S. A.: The international classification for seasonal snow on the ground, UN-ESCO/IHP, Paris, 2009.

Freudiger, D., Kohn, I., Stahl, K., and Weiler, M.: Large-scale analysis of changing frequencies of rain-on-snow events with flood-generation potential, Hydrol. Earth Syst. Sci., 18, 2695–2709, doi:10.5194/hess-18-2695-
280 2014, 2014.

Gray, D. M. and Male, D. H.: Handbook of Snow, The Blackburn Press, Caldwell, New Jersey, 1981.

Grenfell, T. C. and Putkonen, J.: A method for the detection of the severe rain-on-snow event on Banks Island, October 2003, using passive microwave remote sensing, Water Resour. Res., 44, W03425, doi:10.1029/2007WR005929, 2008.

285 Grody, N.: Relationship between snow parameters and microwave satellite measurements: Theory compared with advanced microwave sounding unit observations from 23 to 150 GHz, J. Geophys. Res.-Atmos., 113, 1–17, 2008.

Hirashima, H., Yamaguchi, S., Sato, A., and Lehning, M.: Numerical modeling of liquid water movement through layered snow based on new measurements of the water retention curve, Cold Reg. Sci. Technol., 64,
290 94–103, 2010.

Hobbs, P. V.: Ice Physics, Clarendon Press, Oxford, UK, 1974.

Katsushima, T., Kumakura, T., and Takeuchi, Y.: A multiple snow layer model including a parameterization of vertical water channel process in snowpack, Cold Reg. Sci. Technol., 59, 143–151, 2009.

Keegan, K., Albert, M. R., and Baker, I.: The impact of ice layers on gas transport through firn at the North
295 Greenland Eemian Ice Drilling (NEEM) site, Greenland, The Cryosphere, 8, 1801–1806, doi:10.5194/tc-8-1801-2014, 2014.

Kumpula, J., Parikka, P., and Nieminen, M.: Occurrence of certain microfungi on reindeer pastures in northern Finland during winter 1996–97, Rangifer, 20, 3–8, 2000.

La Placa, S. J. and Post, B.: Thermal expansion of ice, Acta Crystallogr., 13, 503–505, 1960.

300 Langham, E. J.: Phase equilibria of veins in polycrystalline ice, Can. J. Earth Sci., 11, 1280–1287, 1974.

Langlois, A., Royer, A., Derksen, C., Montpetit, B., Dupont, F., and Goïta, K.: Coupling of the snow thermodynamic model SNOWPACK with the Microwave Emission Model for Layered Snowpacks (MEMLS) for subarctic and arctic snow water equivalent retrievals, Water Resour. Res., 48, 819–821, doi:10.1029/2012WR012133, 2012.

305 Lemmetyinen, J., Pulliainen, J., Rees, A., Kontu, A., and Derksen, C.: Multiple-layer adaptation of HUT Snow Emission Model: comparison with experimental data, IEEE T. Geosci. Remote, 48, 2781–2794, 2010.

Lonsdale, D. K.: The structure of ice, P. Roy. Soc. Lond. A Mat., 247, 424–434, 1958.

Marsh, P.: Wetting front advance and freezing of meltwater within a snow cover: 1. Observations in the Canadian Arctic, Water Resour. Res., 20, 1853–1864, 1984.

310 Mätzler, C.: Relation between grain-size and correlation length of snow, J. Glaciol., 48, 461–466, 2002.

Mätzler, C. and Wiesmann, A.: Extension of the microwave emission model of layered snowpacks to coarse-grained snow, Remote Sens. Environ., 325, 317–325, 1999.

Montpetit, B., Royer, A., Roy, A., Langlois, A., and Derksen, C.: Snow microwave emission modeling of ice lenses within a snowpack using the microwave emission model for layered snowpacks, IEEE T. Geosci.
315 Remote, 51, 4705–4717, 2012.

Pan, J., Jiang, L., and Zhang, L.: Comparison of the multi-layer HUT snow emission model with observations of wet snowpacks, Hydrol. Process., 28, 1071–1083, 2014.

Pfeffer, W. T. and Humphrey, N. F.: Determination of timing and location of water movement and ice-layer formation by temperature measurements in sub-freezing snow, J. Glaciol., 42, 292–304, 1996.

320 Picard, G., Brucker, L., Roy, A., Dupont, F., Fily, M., Royer, A., and Harlow, C.: Simulation of the microwave emission of multi-layered snowpacks using the Dense Media Radiative transfer theory: the DMRT-ML model, Geosci. Model Dev., 6, 1061–1078, doi:10.5194/gmd-6-1061-2013, 2013.

Putkonen, J. and Roe, G.: Rain-on-snow events impact soil temperatures and affect ungulate survival, Geophys. Res. Lett., 30, 37, doi:10.1029/2002GL016326, 2003.

325 Rees, A., Lemmetyinen, J., Derksen, C., Pulliainen, J., and English, M.: Observed and modelled effects of ice lens formation on passive microwave brightness temperatures over snow covered tundra, Remote Sens. Environ., 114, 116–126, 2010.

Sihvola, A. and Tiuri, M.: Snow fork for field determination of the density and wetness profiles of a snow pack, IEEE T. Geosci. Remote, GE-24, 717–721, 1986.

330 Takala, M., Luojus, K., Pulliainen, J., Derksen, C., Lemmetyinen, J., Kärnä, J.-P., Koskinen, J. T., and Bojkov, B.: Estimating northern hemisphere snow water equivalent for climate research through assimilation of space-borne radiometer data and ground-based measurements, Remote Sens. Environ., 115, 3517–3529, 2011.

Wiesmann, A. and Mätzler, C.: Microwave emission model of layered snowpacks, Remote Sens. Environ., 70,
335 307–316, 1999.

Ye, H., Yang, D., and Robinson, D.: Winter rain on snow and its association with air temperature in northern Eurasia, Hydrol. Process., 22, 2728–2736, 2008.

Table 1. Measurements of pure ice density, adapted from Hobbs (1974).

Temperature (°C)	Density (kg m^{-3})	Reference
0	916.4	Lonsdale (1958) using diffraction measurements
−30	919.3	
−60	922.7	
−10	918.7	Eisenberg and Kauzmann (1969)
−20	920.3	based on X-ray diffraction measurements
−40	922.8	made by La Placa and Post (1960)

Table 2. Ice layer density measurements, (all values have been corrected to account for the measured $-0.19\,\mathrm{cm}^3$ bias in volume).

Site	n	Mean (kg m^{-3})	SD (kg m^{-3})
CARE – Natural	29	906	17
North Bay – Natural	15	890	21
North Bay – Artificial	15	921	18
Inuvik – Artificial	28	915	26

Table 3. Measurements of ice layer bubble size and ice layer thickness (all sizes in mm). n is number of samples, $n < 0.1$ is the number of bubbles with diameter of less than 0.1 mm.

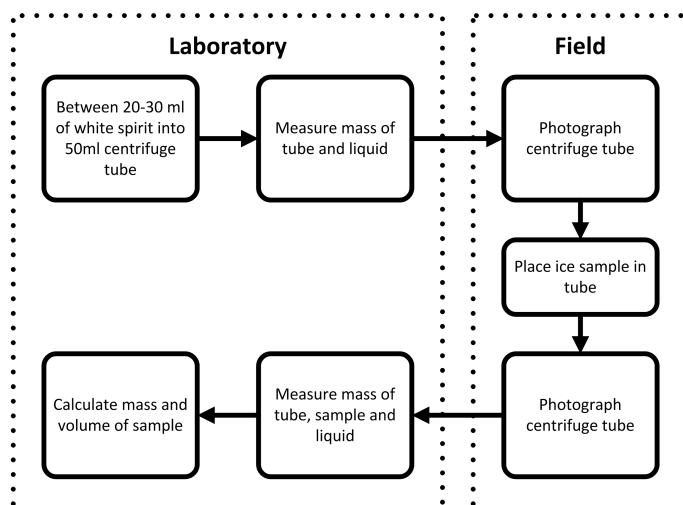|	Type	n	$n < 0.1$	Mean	SD	n	Mean	SD
			Bubble Diameter			Layer Thickness		
CARE	Natural	0	–	–	–	29	8	0.6
North Bay	Natural	14	4	0.16	0.12	15	3	0.6
	Artificial	12	6	0.08	0.03	15	5	0.9
Inuvik	Artificial	0	–	–	–	28	2	0.5
Overall	–		26	10	0.12	0.1	86	5	2.7

Figure 1. Flow chart describing the methodology to measure densities of ice layers from a snowpack.
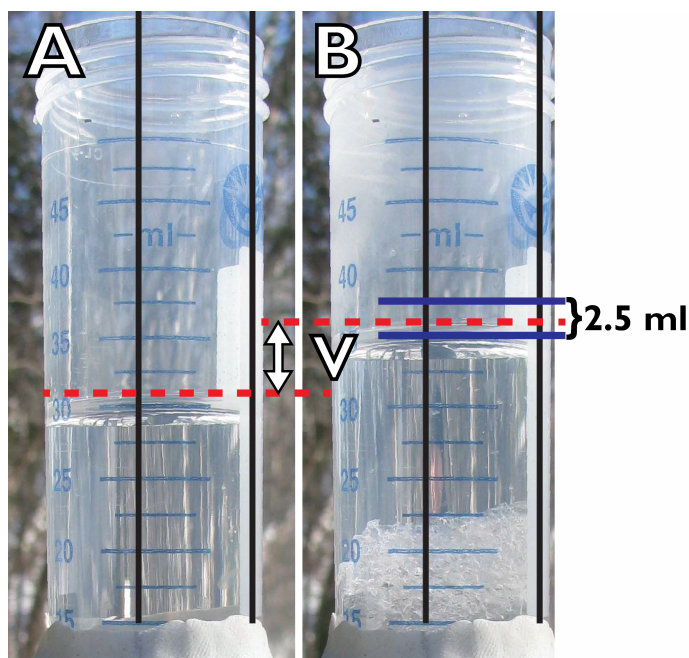

Figure 2. Example of pair of photos used in calculation of ice sample volume. **(a)** taken before the sample was added and **(b)**, taken after. V is equal to the volume of the ice sample. Black lines are guides added to help assess the quality of the photos.
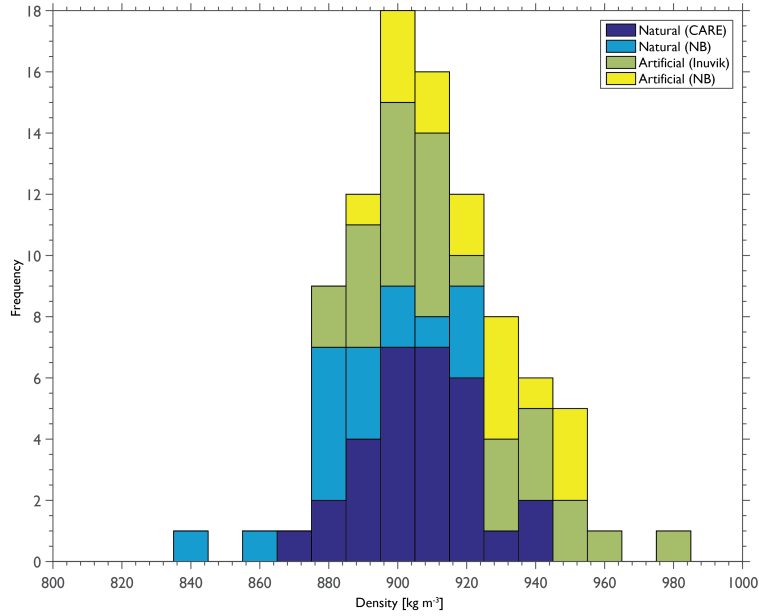
Figure 3. Summary of ice layer density measurements. Stacked histogram showing frequency of each density measurement, colours show distribution of artificial and natural ice layers across multiple sites.
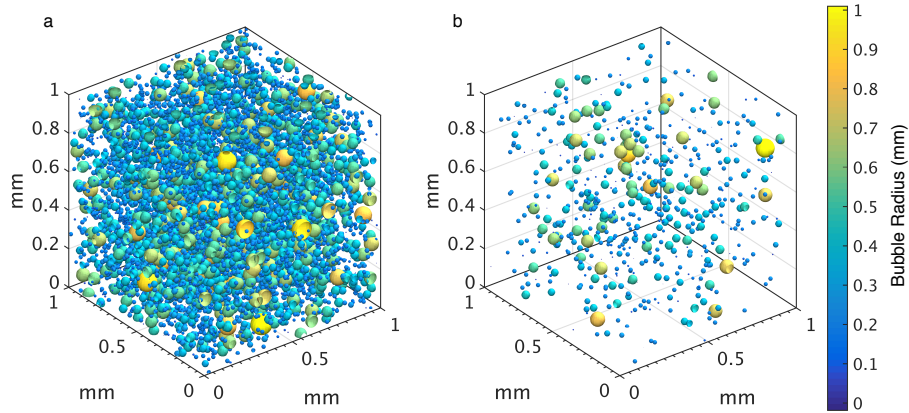

Figure 4. Examples of the numerical representation of ice layers used to investigate porosity, **(a)** shows a sample with simulated density of $800\,\mathrm{kg\,m^{-3}}$ and **(b)** shows a sample with density $909\,\mathrm{kg\,m^{-3}}$.
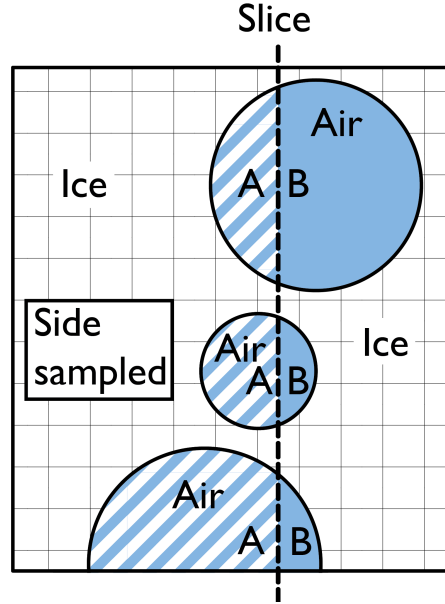
Figure 5. Schematic representation of slicing technique to measure porosity. Air bubbles (shaded in blue) are shown in an ice sample, the theoretical slice was made at the location of the dashed line. The left hand side was chosen as the side to be sampled, and so all of the diagonally striped areas marked "A" were calculated and summed to calculate the overall porosity of the sample.
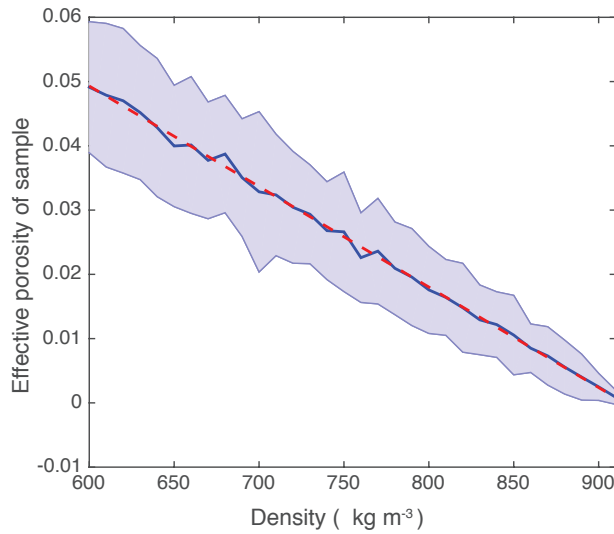

Figure 6. Sample density vs mean simulated sample porosity (Blue line). Sample porosity was calculated at 0.1 cm intervals throughout the sample, shaded area shows mean ± 1 standard deviation. Red dashed fitted linear trend line (Eq. 1) was calculated using a least squares regression.